Wenhao Zhao
Shulin Tian
Lei Huang
Ke Liu
Lijuan Dong

School of Automation Engineering, University of Electronic Science and Technology of China, Chengdu, P.R. China

Received November 30, 2019
Revised January 8, 2020
Accepted January 10, 2020

Review

The review of Lab-on-PCB for biomedical application

Prevention of infectious diseases, diagnosis of diseases, and determination of treatment options all rely on biosensors to detect and analyze biomarkers, which are usually divided into four parts: cell analysis, biochemical analysis, immunoassay, and molecular diagnosis. However, traditional biosensing devices are expensive, bulky, and require a lot of time to detect, which also limited its application in resource-limited areas. In recent years, Lab-on-PCB, which combines biosensing technology and PCB technology, has been widely used in biomedical applications due to its high integration, personalized design, and easy mass production. Among these Lab-on-PCB sensing devices, the PCB circuit plays an important role. It can be directly used as a resistance sensor to count cells, and also used as a control device to automatically control the detection device. Flexible PCBs can be used to make wearable medical biosensors. In addition, due to the high degree of integration of the PCB circuit, Lab-on-PCB can perform multiple inspections on the same platform, which reduces the inspection time equivalently. Therefore, in this review paper, we discuss the application of Lab-on-PCB in four analysis methods of cell analysis, biochemical analysis, immunoassay, and molecular diagnosis, and give some suggestions for improvement and future development trends at the end.

Keywords:
Biosensor / Lab on PCB / Microfluidics sensor / Micro-TAS
DOI 10.1002/elps.201900444

1 Introduction

The occurrence of diseases is often accompanied by abnormal changes in the concentration of certain substances in the human body, so the rapid and effective detection of disease-related biomarkers is a powerful guarantee for disease prevention, disease treatment, and disease control [1–5]. Although traditional medical detection equipment can perform very accurate detection of medical samples (such as blood, urine, and living tissue), these devices often require complicated operation procedures and long detection times [6–8]. And in the course of disease treatment, multiple detections are needed to adjust the treatment plan in time. It will take a lot of time and is not suitable for today's fast-paced life.

In 1996, Lammerink et al. first proposed the concept of Lab-on-PCB that integrates microchannels, sensors, and other components on a printed circuit board (PCB) [9]. With the continuous improvement of the performance of micro-biosensors and the rapid development of PCB manufacturing industry, the Lab-on-PCB biomedical detection device has been the focus of attention. PCB technology has the following advantages: (a) PCB-based circuit design has great flexibility and can be customized according to specific remands. (b) The application of PCB technology allows the integration of electronic modules and sensing modules on the same platform, which can effectively reduce the size of the device while ensuing the accuracy of detection. (c) The standardized and mature PCB manufacturing process enables PCB-based detection devices to be manufactured on a large scale that reduce the cost efficiently. (d) The development of flexible PCB technology has promoted the development of wearable detection devices. Therefore, in the past decade, there have been a lot of reports on the application of Lab-on-PCB to various biomedical applications. In addition, we did a survey via searching the keywords of "Printed-circuit-board and biomedical" in the four well-known international databases of IEEE, Springer, Elseviser, and Wiley. The results are as shown in Fig. 1 that the research on Lab-on-PCB for biomedical have gradually increased in the past decade. Especially in the last 2 years, it has received great attention. According to different detection methods and analysis principles, these biomedical applications can be divided into four categories: (1) cell analysis based on Coulter's counting principle and cell imaging technology for analysis of red cells, white cells, and tumor cells [10–16]; (2) biochemical analysis based on

Correspondence: Professor Ke Liu, School of Automation Engineering, University of Electronic Science and Technology of China, Chengdu 611731, P.R. China
E-mail: liuke@uestc.edu.cn

Abbreviations: **CMOS**, complementary metal-oxide-semiconductor transistor; **HUVEC**, human umbilical vein endothelial cells; **IDT**, interdigital transducer; **PCB**, printed circuit board; **RBC**, red blood cell

Color online: See article online to view Figs. 1–11 in color.

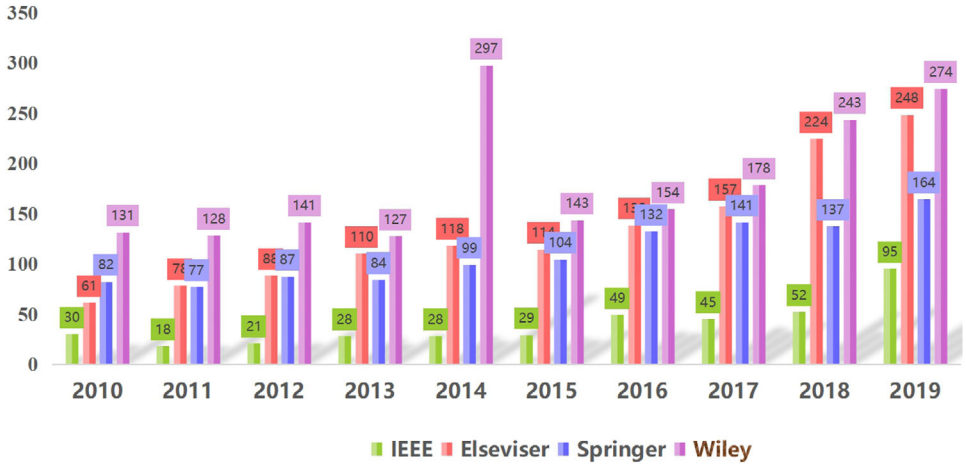

Figure 1. The statistical data on research about Lab-on-PCB for biomedical applications.

various enzyme reactions for analysis of blood glucose, electrolytes, and other nutrients in the human body [17–20]; (3) immunoassay based on antigen–antibody specific reaction [21–24]; and (4) molecular diagnosis based on PCR [25–29] for analysis of different kinds of nucleic acid. In these applications, PCB-based circuits are used as cell sensors for cell counting; as electrochemical sensors for electrochemical analysis of blood glucose, electrolytes, and other nutrients in the human body; as a controller to control the sensing system; and as a data processing center to convert and transfer the detection data. Furthermore, it can establish a comprehensive mobile detection platform by integrating communication modules such as Bluetooth, near-field communication, USB interface, or OTG interface on the PCB to connect with smartphones or mobile electronic devices [30].

In this paper, we will review the recent works on Lab-on-PCB for biomedical applications. Four types of biomedical applications were classified according to the different detection methods as cell analysis, biochemical analysis, immunoassay, and molecular diagnosis. We will introduce the Lab-on-PCB for various biomedical applications in detail from the structure, performance, and application background. Finally, we discuss the current limitations and associated challenges in the end and give some future perspectives for this promising technology.

2 Cell analysis

As an important part of the human body, cells are closely related to health. We can evaluate a person's physical status by counting cells or observing the morphology of cells. For example, the white blood cell count is an important health indicator, and the number of white blood cells will be abnormal when fighting infections from bacteria and viruses [31]. As another example, during cancer metastasis, tumor cells need to enter the bloodstream through microvessels. Accordingly, isolating and detecting tumor cells in peripheral blood has become an effective method for the early diagnosis of cancer metastasis [32]. But the early traditional cell experiments used only standard benchtop instruments, making cell analysis only allowed to be performed in professional laboratories [33–36]. Recently, many researchers use PCB-based resistance sensors or capacitive sensors to build a Lab-on-PCB platform to count cells or detect cell viability for disease diagnosis and drug toxicity detection in a low-cost and mini-size way [37–43].

2.1 Lab-on-PCB for counting cell

Guo et al. designed a microfluidic cytometer on an SU-8 coated PCB for rapid detection and enumeration of rare cells [44]. This cytometer is based on Coulter principle; when the microparticles pass through the sensing hole of the Coulter counter, the impedance will change due to the blockage, and then a current pulse can be detected. And the amplitude of the impedance pulse will increase as the size increase of the microparticles. According to the detection results of specific concentrations of Hela cells by the commercial cytometer and the proposed device, the accuracy of counting the tumor cells of the proposed device is comparable to the commercial cytometer. Furthermore, this device has a great advantage in price due to the cheap PCB.

A year later, Guo et al. improved the PCB-based microfluidic cytometer, using a cover slip as a dielectric layer that allows AC signals to detect the impedance changes of microfluidic channels [45]. The detection results of Hela cells and human red blood cells (RBCs) showed that the Hela cells could be detected by the AC signal in which the frequency is above 400 kHz, but the RBC cells could not be detected. The average diameter of Hela cell is 16 μm and the average diameter of RBCs is 5 μm. Therefore, the improved cytometer not only has high detection accuracy but also has good cell selectivity. These advantages make it a great prospect in the application of tumor metastasis diagnosis.

In addition, Guo et al. proposed a PCB-based on-demand microfluidic single-cell imaging device that combines single-cell imaging and differential-resistance pulse sensing to extract the specific size cells' morphological information

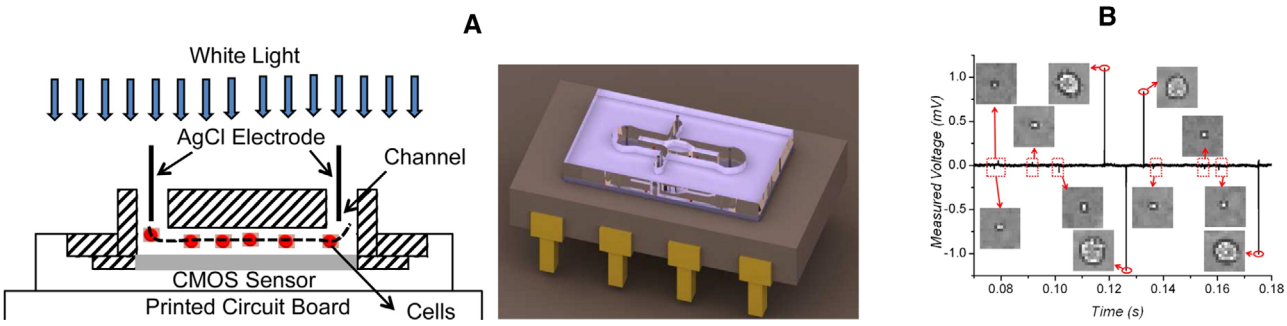

Figure 2. (A) Image of PCB-based on-demand microfluidic single-cell imaging device and (B) the cell image captured by the proposed device, reprinted with permission from [46]. Copyright 2015 American Chemical Society.

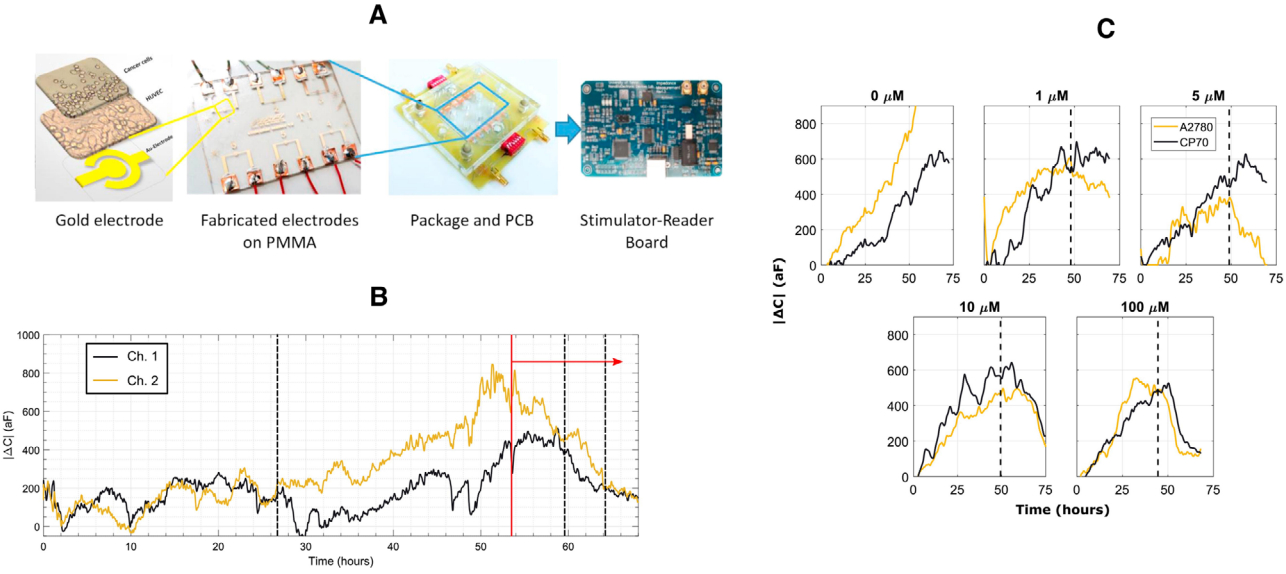

Figure 3. (A) An impedance sensor on PCB consists of an impedance change reaction plate and an impedance change reading plate, reprinted with permission from [47]. Copyright 2018 Elsevier; (B) and (C) the results of proposed cell viability detection devices [48]; (B) the detection result of the effects of cisplatin on human ovarian cancer cell; (C) the detection results of different doses of drugs on different drug-resistant cells, reprinted with the permission from [48]. Copyright 2019 Elsevier.

such as the shape, texture, and intracellular structure [46]. It has been confirmed in previous studies that different sizes of cells will produce different amplitude pulse signals when they pass through the sensing hole. A control circuit is designed on the PCB, which will quantize the pulse signal via analog-to-digital chip and transmit the digital data of amplitude to Field Programmable Gate Array. If the data are within the set threshold, the Field Programmable Gate Array will generate an enable signal to excite the Complementary Metal-Oxide-Semiconductor Transistor (CMOS) sensor, which is in snapshot mode to capture the image of the passing cell. The threshold voltage was set to 0.4 mV and the mixture of RBCs and HepG2 cells was detected by the proposed device. Figure 2A shows the pulse signal generated by a series of cells passing through the sensing hole, and the cells' images captured by the CMOS were attached. From Fig. 2B, we can see that if the threshold voltage is set to be higher than maximum pulse amplitude induced by RBCs, the HepG2 cells can be imaged on-demand. Therefore, the proposed device can effectively count cells and image the cells that we are interested in, demonstrating powerful selective single-cell imaging capabilities.

2.2 Lab-on-PCB for detecting cell viability

Nikshoar et al. designed an impedance sensor on PCB for detection of populated metastatic cancer cells from primary ones based on a recently reported metastatic diagnosis assay [47]. As shown in Fig. 3A, the sensor consists of an impedance change reaction plate and an impedance change reading plate. The human umbilical vein endothelial cells (HUVEC) are cultured on the sensing electrodes, which are integrated on a poly-methyl methacrylate substrate in six circular microelectrode arrays. When the metastatic cancer cells invade the HUVEC on the electrodes, it will cause the HU-

Table 1. Lab-on-PCB for biomedical applications

Analyte	Size	Role of PCB	Performance	Characteristic	Reference
Na^+ in sweat	61 × 25 × 1.2 mm	Reader device	Range: 10–90 mM Accuracy: ±5 mM@50 mM	Wearable	Daniel et al. (2015) [49]
Cholera toxin in blood	Litter than a mice	Sensor and reader device	LOD in vitro test: 50 pM LOD in vivo test: 1.6 nM	Wearable and invade	Na et al. (2019) [50]
Glucose and lactate levels in sweat	50 × 24 mm	Reader device	Lactate RSD: 1.2% Glucose RSD: 1.6% LOD: 50 μM	Wearable	Martin et al. (2019) [52]
Tetramethybenzadine (TMB)	About 45 × 52 × 2.8 mm	Sensor and reader device	There is a clear correlation between the concentration of TMB and magnitude of signal	Drop the solution on the device	Vasilakis et al. (2016) [20]
Glucose and lactate in brain	32 × 18 mm	Reader device	Glucose:0.4 ± 0.1 mM Lactate:0.6 ± 0.15 mM	Wearable and invade into brain	Rocchitta et al. (2013) [53]
Glucose in sweat	Head band	Sensor and reader device	RSD: 3.2% LOD: 2 μM	Wearable	Zhu et al. (2019) [57]
Na^+, K^+, Cl^-, and pH in sweat	PCB: 4 × 8 mm Sensor: 3 × 3 mm	Reader device	Be able to detect multiple parameter at the same, and reflect the changing relationship between them	Wearable	Nyein et al. (2018) [60]
Uric acid in blood	50 × 70 mm	Sensor and reader device	CV: Low concentration (<200 μmol/L): 4.56% Mid concentration (201–435 μmol/L): 2.66% High concentration (>436 μmol/L): 1.83%	Combined with smartphone	Guo et al. (2016) [65]
β-Ketone in blood	A dongle smaller than a smartphone	Sensor	CV: 3.79%	Combined with smartphone	Guo et al. (2017) [66]
Alcohol in blood	38.5×22.5 mm	Reader device	Limit of detection: 1.35 nA Limit of quantification: 4.5 nA	Combined with smartphone	Aymerich et al. (2018) [67]

VEC to retract and detach from the electrodes, which will cause a large change in impedance. And the primary cancer cells cannot invade the HUVEC. Finally, the impedance response reader is used to monitor the impedance before and after the addition of cancer cells.

Senevirathna et al. proposed a PCB-based capacitive biosensor for automated, real-time, and label-free monitoring of cell viability [48]. As cell proliferation and tight binding to the substrate regulate the dielectric properties of the cell–substrate interface, cell proliferation can be measured by measuring changes in surface capacitance. At the same time, time-lapse optical imaging of the sensor surface was added to observe cell growth to verify the measurement results. As shown in the experimental results of Fig. 3B, a 100 μm dose of cisplatin was added to the growth wells of two human ovarian cancer cells cultured for 48 h, and it was found from the experimental images and data 4 h later that the cells began to die. In addition, they did another set of experiments to show the effect of drug dose on the viability of different drug-resistant cells, as shown in Fig. 3C. Therefore, the proposed PCB-based biosensor can greatly help drug development because of its excellent performance for cell viability monitoring.

3 Biochemical analysis

The electrochemical analysis is the use of catalytic enzymes or other catalytic methods to cause the analyte to react with other reactants to produce a measurable electric signal. It is usually used to detect the concentration of some health indicators such as energy substances (glucose), electrolytes (K^+, Na^+, Cl^-, pH), and metabolites [49–51]. In addition, the electrochemical sensor directly converts the detected information into electrical signals that can be processed and transmitted by the circuit. Therefore, with the assistance of flexible circuit board and integrated circuits, the electrochemical sensor can be made into wearable sensing devices or integrated into smartphones, which lead the development trend of recently biomedical applications (Table 1).

3.1 Lab-on-PCB for detecting glucose

Due to the personalization and miniaturization of PCB circuits, Martin et al. proposed a wearable biomedical device for real-time detection of glucose in sweat [52]. This device consists of an epidermal microfluidic detection platform that

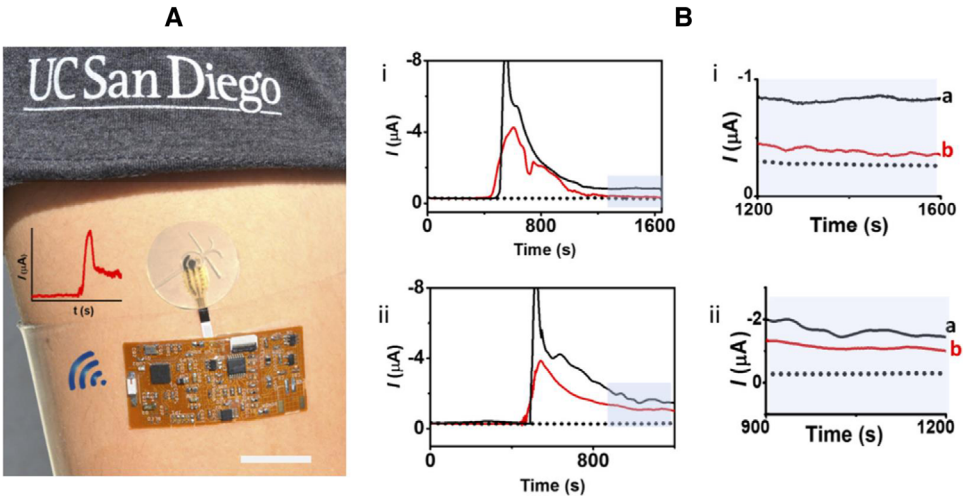

Figure 4. (A) The sketch of a wearable detection biomedical device for real-time detection of glucose in sweat and (B) the detection results of before and after meals, reprinted with permission from [52]. Copyright 2017 American Chemical Society.

is manufactured by a combination of lithography and silk printing technology to collect sweat from the skin surface, and a flexible electronic board for real-time wireless data transmission via Bluetooth (Fig. 4A). An electrochemical biosensor modified with glucose oxidase is integrated into the epidermal microfluidic detection platform. When glucose in the sweat reacts with glucose oxidase on the electrode to generate hydrogen peroxide, the current in the circuit will increase. And the magnitude of the current is related to the glucose concentration. As shown in Fig. 4B, there is a significant difference in the glucose content before and after meals (red lines indicate before meals, black lines indicate after meals). The device has a great development prospect in noninvasive monitoring of glucose concentration in human body, which can bring great convenience and assistance to the recuperation of diabetic patients.

In addition, Rocchitta et al. proposed a PCB-based telemetry system for simulataneous detection of extracellular glucose and lactic acid in the brain [53]. The Pt/Ir cylindrical electrode modified by glucose oxidase and lactate oxidase was implanted into the right striatum and left striatum of the mice by stereotactic surgery. As shown in Fig. 5A, the electrodes were connected with the double-sided PCB fixed on the top of the mice, and a microvibration sensor is integrated into the PCB circuit to record the movement of the mice. From the experimental data, the device accurately records the relationship between mice motion and brain neurochemistry. When the motion increased, the concentration of glucose decreased with the increase of lactic acid in the mice's brain. When the mice calmed, the concentration of glucose gradually increased. This method of simultaneously recording brain neurochemistry and animal motion provides inspiration for the researcher of motion-related diseases such as Parkinson's syndrome.

There are many other researches on electrochemical sensors for the detection of lactic acid and glucose in humans based on the corresponding oxidoreductases [54–56]. However, the accuracy and sensitivity of the detection of such biosensors will be influenced in the case of long-term unsteady physiological conditions and enzymes sensitive to environmental conditions (such as pH and temperature). Zhu et al. presented a nonenzymatic electrochemical sensor based on electrochemical water splitting-assisted electrocatalysis to solve this problem [57]. Their wearable electrochemical sensors are shown in Fig. 5B, which integrated a metal–organic frameworks based electrode and flexible PCB-based data acquisition and emission device. First, a high negative potential is necessary for inducing the decomposition of water molecules on the surface of the electrode to produce hydroxide ions to make an alkaline environment for metal–organic frameworks electrode to catalyze the oxidative decomposition of glucose. And then a moderate potential is applied to catalyze the redox reaction of glucose in the sweat, and the collected electrical signals are sent to the smartphone for analysis via Bluetooth. Finally, the positive potential is applied to clean the electrode in preparation for the next detection. It was confirmed by experiments (Fig. 5C) that the concentration of glucose in the sweat measured by the proposed sensor showed a strong correlation with the blood glucose concentration measured by the commercial blood glucose meter. Furthermore, the glucose concentration in the sweat samples was analyzed using HPLC-MS, and the results were consistent with those obtained with the proposed sensor.

3.2 Lab-on-PCB for detecting electrolytes

Measurement of various electrolytes in the human body is also indispensable, playing a very important role in tissue ischemia assessment, dehydration assessment [58], and other applications. Anastasova et al. proposed four electrochemical sensing platforms based on PCB technology for detecting various parameters such as Na^+ ions, K^+ ions, and pH. The pictures of these platforms are shown in Fig. 6; they are divided into two rigid platforms for in vitro liquid sample measurement and two flexible platforms for postoperative intestinal tissue testing [59]. To demonstrate their detection performance, the detection results of the four platforms

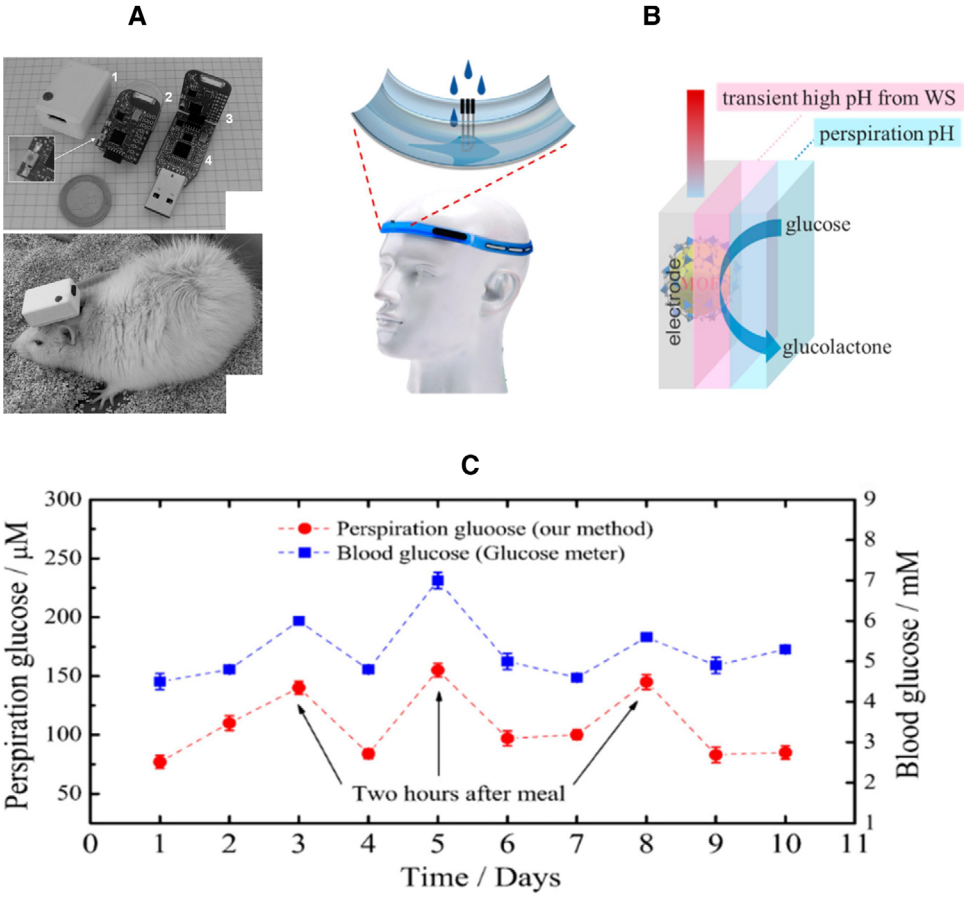

Figure 5. (A) The picture of a PCB-based detection biomedical device; this device can be inserted into the brain of mice to detect the extracellular glucose concentration and lactate concentration, reprinted with permission from [53]. Copyright 2013 American Chemical Society, (B) the structure of a head-mounted nonenzymatic biochemical sensor to detect the glucose concentration in the sweat, and (C)the detection results of proposed devices and the detection results of commercial device, showing good agreement, reprinted with permission from [57]. Copyright 2019 American Chemical Society.

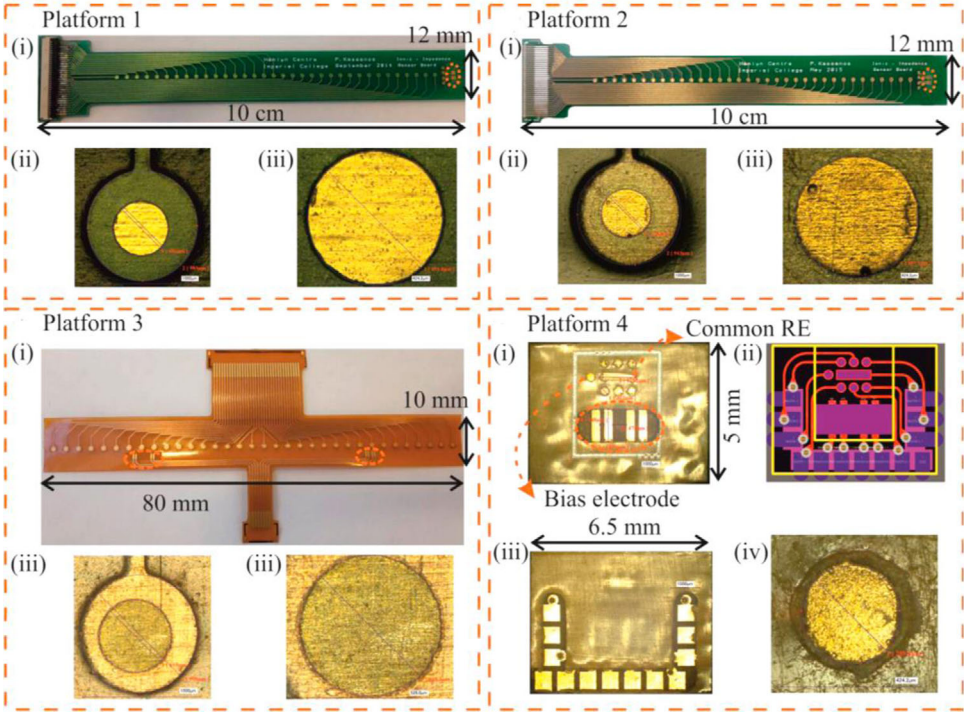

Figure 6. Four kinds of biochemical sensors for detecting the electrolytes in human body based on PCB technology, which are divided into two rigid platforms for detection in vitro (the first and second) and two flexible platform for detection in vivo (the last two), reprinted with permission from [58]. Copyright 2018 Elsevier.

Table 2. The performance of four platforms

Platform	Analyte	Sensitivity (mV/log)	%RSD	Intercept (mV)	%RSD	Response time (s)	LOD	Drift (mV/24 h)
Platform 1	Na^+	22.2 ± 1.9	4.5	186.1 ± 3.5	3.7	300	10^{-4} M	28.9
Platform 2	Na^+	54 ± 1.5	2.5	241.5 ± 2.3	1.2	200	10^{-4} M	23.2
Platform 3	Na^+	55.8 ± 1.2	3.2	251.3 ± 3.2	1.3	150	10^{-4} M	17.6
Platform 4	Na^+	56.3 ± 0.9	2.5	250 ± 4.2	0.6	30	10^{-5} M	16.5
Platform 1	K^+	22.2 ± 4.9	5.4	186 ± 3.5	4.1	300	10^{-4} M	28.6
Platform 2	K^+	54 ± 2.5	3.5	241.5 ± 2.3	1.9	250	10^{-4} M	32.4
Platform 3	K^+	55.8 ± 1.2	2.4	249.3 ± 2.4	2.5	180	10^{-4} M	24.8
Platform 4	K^+	57.4 ± 1.9	1.9	250 ± 4.2	2.9	40	10^{-5} M	19.6
Platform 1	H^+	–25.6 ± 1.6	3.5	161.3 ± 3.5	2.8	150	3.5 units	26.5
Platform 2	H^+	–59 ± 1.8	2.2	116.9 ± 2.3	1.1	50	2.6 units	20
Platform 3	H^+	–69.8 ± 0.8	3	116 ± 2.8	1.2	30	3.5 units	10
Platform 4	H^+	–73.4 ± 0.6	2.6	118 ± 4.5	0.9	10	2.4 units	4.2

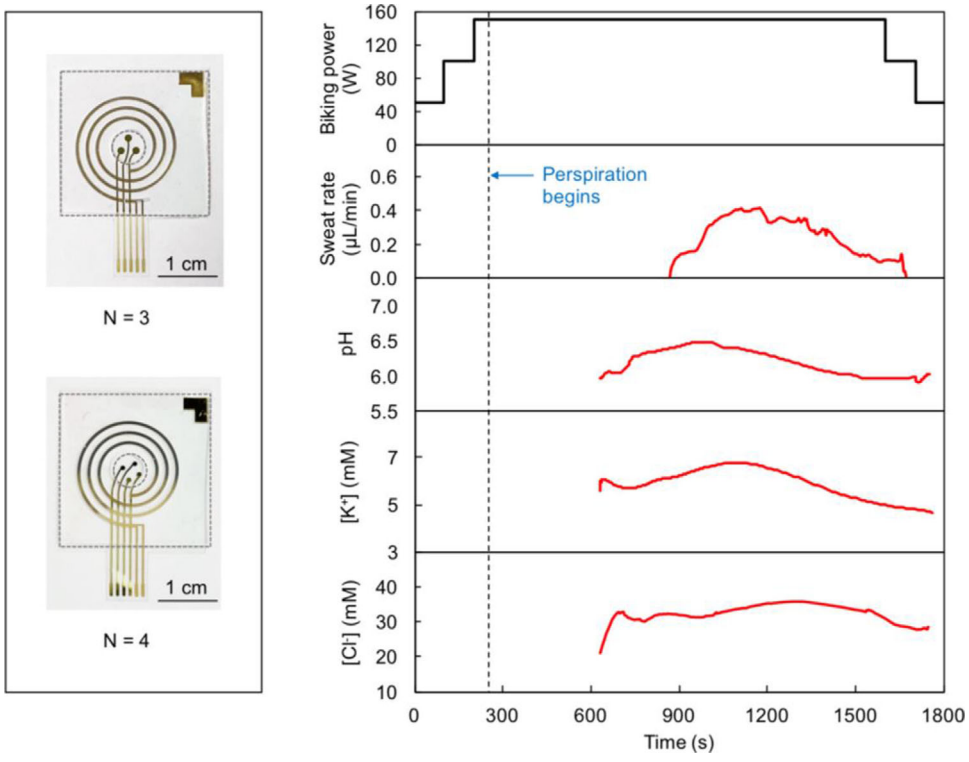

Figure 7. A multiple detection device based on PCB technology and microfluidic for electrolytes and the detection results, reprinted with permission from [60]. Copyright 2018 American Chemical Society.

for saliva samples are shown in Table 2. The flexible hard gold platform 4 exhibits the best performance with the high sensitivity as large as 73.4 mV/pH, 56.3 mV/log [Na+], and 57.4 mV/log [K+]. Although platform 1 which is rigid with electroless nickel immersion gold finish has the worst performance, it has the lowest cost and simple production method that makes it is suitable for large-scale and low-cost production. This advantage makes it effective for use in developing worlds and paves the way for the decentralization of healthcare in developed countries.

Nyein et al. proposed a PCB-based microfluidic wearable sensor platform that can be used to analyze the concentration of various electrolytes in sweat and simultaneously detect the rate of sweating, providing a platform for comprehensive analysis of sweat secretion [60]. An electrochemical sensor for sweat electrolyte analysis and an electrical impedance rate sensor for sweat rate analysis are integrated into the microfluidic channel, and $Na^{+,}$ K^+, Cl^-, pH, and sweat rates can be simultaneously detected by incorporating different electrochemical sensing electrodes. As shown in Fig. 7, each electrode corresponds to an analytical detection of a substance. And the analysis results are consistent with previous studies [61–64] that about 10 min after sweating, sweat enters the fluid channel, and then the sweating rate gradually

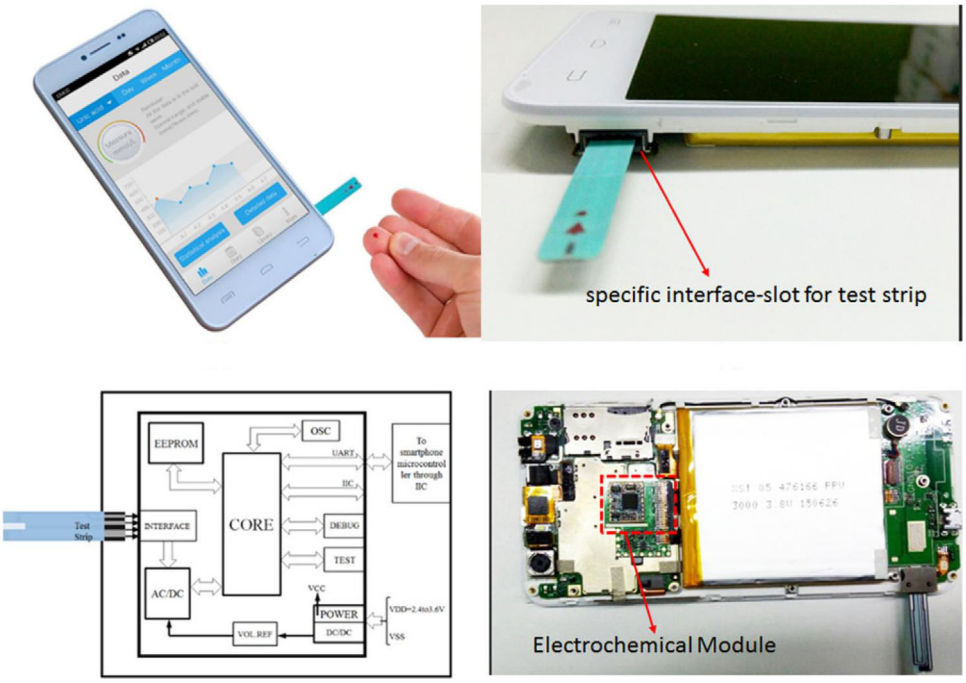

Figure 8. Photograph of the proposed medical smartphone based on PCB technology for UA detection in human blood samples, reprinted with permission from [65]. Copyright 2016 American Chemical Society.

increases and returns to the original state after about 20 min. The sweat pH and Cl^- show similar trends as the sweat rate.

3.3 Lab-on-PCB combined with a smartphone for electrochemical analysis

Recently, with the development and popularization of smartphones, Lab-on-PCB has brought benefits to PCB-based electrochemical sensors. The electrochemical sensor is made into an electronic dog or integrated into the smartphone to connect with the smartphone by PCB technology. Thanks to the excellent computing performance and communication capabilities of smartphone, the detection data collected by electrochemical sensors can be quickly analyzed and uploaded to the personal monitoring healthcare center and the online personal clinic via smartphone. For example, Guo et al. reported the world's first medical smartphone for uric acid detection [65]. As shown in Fig. 8, a PCB-based electrochemical module is integrated inside the smartphone, and the electrochemical module passes through a specific interface connect with an external disposable electrochemical uric acid test strip. Only one drop of 30 μL of whole blood can be used to detect the concentration of uric acid in peripheral blood. Their group also proposed an electrochemical biosensor that uses an electronic dog to connect to a normal smartphone to detect concentration of blood β-ketone [66]. An electronic dog based on PCB technology is used to receive the detection signal of the concentration of blood β-ketone from the electrochemical ketone test strip, which is then sent to the smartphone to analysis and management only needs to download a special application on the smartphone. With the assistance of this PCB-based electronic dog, the normal smartphone can also easily be used to monitor people's health that makes the medical dog to have great applicable potential in mobile health applications.

In addition, Aymerich et al. also proposed a method for detecting ethanol intoxication in whole blood samples in combination with a normal smartphone and a PCB-based electronic medical dog [67]. The smartphone powers the PCB through the USB interface, enabling it to operate the sensor in three modes: potentiostatic, cyclic voltammetry, and chronoamperometry. The op amp-based negative feedback circuit and the microcontroller-based control circuit optimize the redox signal detected by the microfluidic sensing device, and they are integrated compactly on the PCB through the original circuit topology to reduce the size of the electronic dog. And its performance is comparable to that of large and expensive commercial benchtop devices. The experimental results show that the sensitivity of the platform to the ethanol concentration in the whole blood sample reaches 36 nA/g/L in the range of 0–1.25 g/L and the limit of quantification reaches 4.5 nA.

4 Lab-on-PCB for immunoassay

Immunoassays have become a standard technique for diagnosing heart disease, kidney disease, hepatitis, and other infectious diseases [68–72]. And Lab-on-PCB for immunoassay has greater advantages because of the low cost and high integration of PCB. We can integrate multiple sensors on a PCB, which can achieve multiple detections or multiple channels to detect the same sample to improve the accuracy of detection.

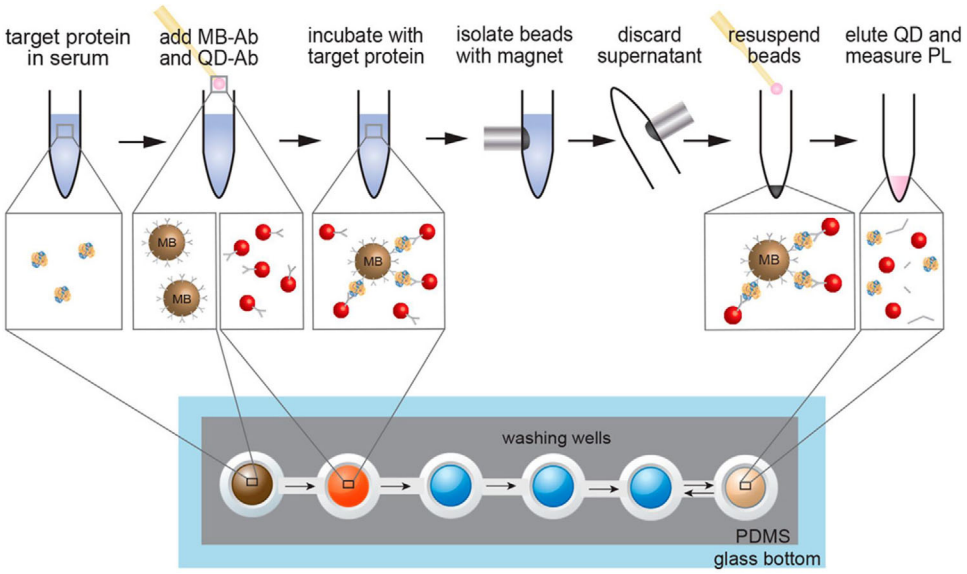

Figure 9. The process of immunoassay of malaria which can perform in "pipelined" mode under the control of PCB circuit, reprinted with permission from [79]. Copyright 2017 American Chemical Society.

Lee et al. presented a surface acoustic wave sensor designed on a PCB board, which can be used to detect cardiac markers [73]. The sensor consists of four interdigital transducer electrode pairs, a frequency counter, and two multiplexers. The finger pairs and width of the electrode determine the center frequency of the signal. When the cardiac marker is captured by the corresponding antibody on the SiO_2 guiding layer between the electrodes, it will cause a change in the output frequency, and the content of the corresponding cardiac marker can be estimated by the frequency change value. At the center frequency of 200 MHz, the three heart markers of cTnl, CK-MB, and myoglobin are detected, and the minimum detectable concentrations were 50 pg/mL, 1.1 ng/mL, and 16.0 ng/mL, respectively.

Bonila et al. also proposed a method for immunoassay based on PCB-based electrode arrays [74]. The difference is that they detect analytes by analyzing changes in array impedance. Their detection relies on the ability of urease to produce an increase in conductivity by hydrolyzing the urea substrate. Furthermore, in this method, the enzymatic reaction does not occur on the electrode array, but on a regular glass slide. The performance of the method was evaluated by microarray of mouse universal protein to confirm its detection limit of 0.1 μg/mL. Compared with the method in which the enzymatic reaction directly occurred on the electrode array, the detection limit was not very high. However, due to its flexibility in replacing the microarray, it can be well applied to multiple analysis systems.

Cortisol, a "stress hormone," has been identified as a biomarker that can detect psychological stress [75]. The link between elevated cortisol levels in saliva and anxiety has been identified, but there is a lack of a fast and effective method for detecting cortisol levels under the situation without large laboratory equipment and extensive expertise [76]. Khan et al. proposed a label-free paper-based electronic biosensor chip [77]. A low-cost, reconfigurable small control circuit based on PCB is used to quantify the impedance of the DTSP/SAM/Au electrode before and after the cortisol reacts with the antibody cortisol, which is attached to the electrode. According to the detection results of six standard samples with the known concentration of cortisol and eight saliva samples from volunteers, the detection range of the proposed sensor chip is 3 pg/mL to 10 μg/mL, and the detection limit is 3 pg/mL. And due to the small size of the PCB-based control circuit, it can be easily integrated into a handheld device, and the detected data can be shared via the wireless network.

Nagy et al. proposed a CMOS sensor array integrated circuit implemented on a PCB that can perform multiple immunoassays [78]. The front side of the PCB has a 16*16 COMS array of 256 CMOS sensors covering a layer of SU-8 photoresist modified with antigen or antibody bioprobes. When the bioprobe reacts with the analyte, it will affect the amount of light reaching the lower CMOS sensor, which determines the voltage generated by the sensor. The voltage of 256 sensors can be measured and sent to the smartphone for analysis through the ARM data acquisition platform on the back of the PCB. And using the advanced inkjet printing technology enables each sensor to perform different immunoassays, greatly improving the ability of multiple detections. It can also be obtained by averaging by using more sensors to detect the same object. From the results in Fig. 9A, it can be seen that the proposed device can easily distinguish whether the sample contains rabbit anti-mouse antibody or HIV antibody. The detection limit of HIV antibody concentration is 10 μg/mL, which is far superior to the commonly found in infected population (300–500 μg/mL).

In addition, the flexibility of the PCB circuit can also bring more convenience to immunoassay devices. For example, Kim et al. used a PCB-based electromagnetic coil array to create a "pipelined" immunodetection device to detect malaria [79]. As shown in Fig. 9B, the entire probing process includes capture, marking, two washes, and measurements.

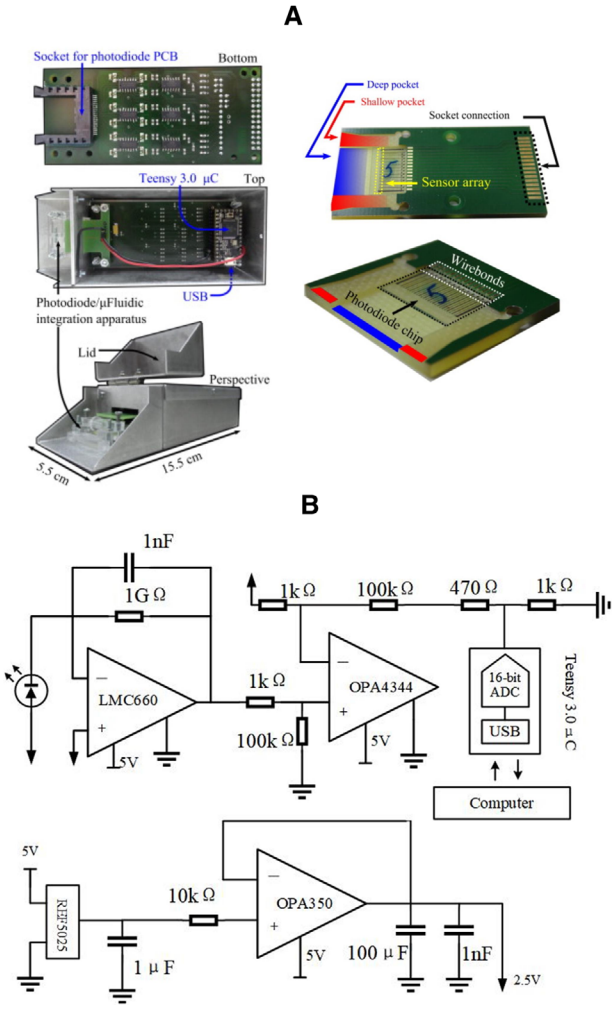

Figure 10. (A) Due to the flexibility of PCB-based circuit, the proposed immunoassay device can easily change the microfluidic channel plate to detect various analytes, and 12 parallel amplification and quantization circuits' schematic diagram is shown in (B), reprinted with permission from [78]. Copyright 2014 Elsevier.

Coils are used on the PCB to achieve automatic translation and mixing of immunomagnetic beads in wells by electromagnetic induction. The method saves a lot of labor costs, and compared to conventional immunoassays and molecular analysis tools, the device is small in size and does not require complicated professional operations, so that it can be effectively utilized in resource-poor environments.

In addition, Novo et al. proposed a "plug-in" immunodetection device and performed an immunoassay of an IgG/anti-IgG model to demonstrate the detection performance of the proposed device [80]. The device consists of a photodiode PCB, a control/amplification circuit PCB, and a microfluidic channel board. The photo of the control/amplification PCB is shown in Fig. 10A. On the top side, there is a microprocessor with a USB interface that can be connected to computer or smartphone. And the bottom side is composed of 12 parallel amplification/quantization circuits (Fig. 10B) and a slot for connecting the photodiode PCB. The structure of the photodiode PCB is as shown in Fig. 10A, and there are two deep pits and one shallow pit on the left side for placing the photodiode chip and the microfluidic channel plate, and the right side is a socket connector. With the assistance of this slotted design, the photodiode PCB can be easily removed for replacement of the microfluidic module to achieve different functions immunoassay, which can greatly save the cost of immunoassay.

5 Molecular diagnosis

The PCR is a temperature-mediated enzyme-catalyzed reaction that mimics the process of DNA replication in nature and exponentially amplifies little DNA or RNA. It is an effective way for molecular diagnosis, therefore PCR-based analysis devices have been widely reported [81–84]. With the assistant of PCB technology, Lab-on-PCB can achieve sample-to-answer PCR analysis, greatly simplifying the complexity of molecular diagnostics.

To address the difficulty of detecting HIV-1 proviral DNA in infants in resource-limit settings, Jangam et al. developed a low-cost, highly integrated sample-to-answer PCR system [85]. We simply collected 100 μL of blood from the baby's heel and used the sample introduction module to separate and extract the DNA from the blood, and then detection result was provided by the proposed system. All this is attributed to the microprocessor on the PCB, under which the system automatically performs the process of reagent transfer, thermal cycling, fluorescence detection, and gives the final result. The results of tests on 5000 blood samples with HIV-1 provirus confirmed that the system can detect HIV-1 in the blood. Although its analytical sensitivity is not as good as that of the laboratory, the system is low in cost and can obtain a detection result rapidly without complicated operation and can provide a preliminary detection for infants in resource-poor areas.

In addition, malaria is a transmission disease caused by malaria parasites, mainly in areas with low incomes and underdeveloped health care. In these areas, medical resources are also in short supply, therefore a low-cost and rapid detection device for control of malaria is essential. For areas with high malaria transmission, microscopy and immunological rapid diagnostic tests have shown excellent performance. However, the two methods are too stretched for the detection of low concentrations of parasites, therefore Choi et al. proposed a sample-to-answer nucleic acid testing device for inexpensive and lower concentration parasite density malaria detection [86]. As shown in Fig. 11A, the operation of the whole device is controlled by a custom microcontrol unit based on PCB. After the detection sample is placed, the device will automatically complete DNA separation and extraction, DNA amplification, fluorescence detection, and data recording. Finally, the results are displayed directly on the LCD screen and the results are recorded on a nonvolatile memory card. The device has four parallel detection units with a test time of 50 min, so the average detection time is 12.5 min.

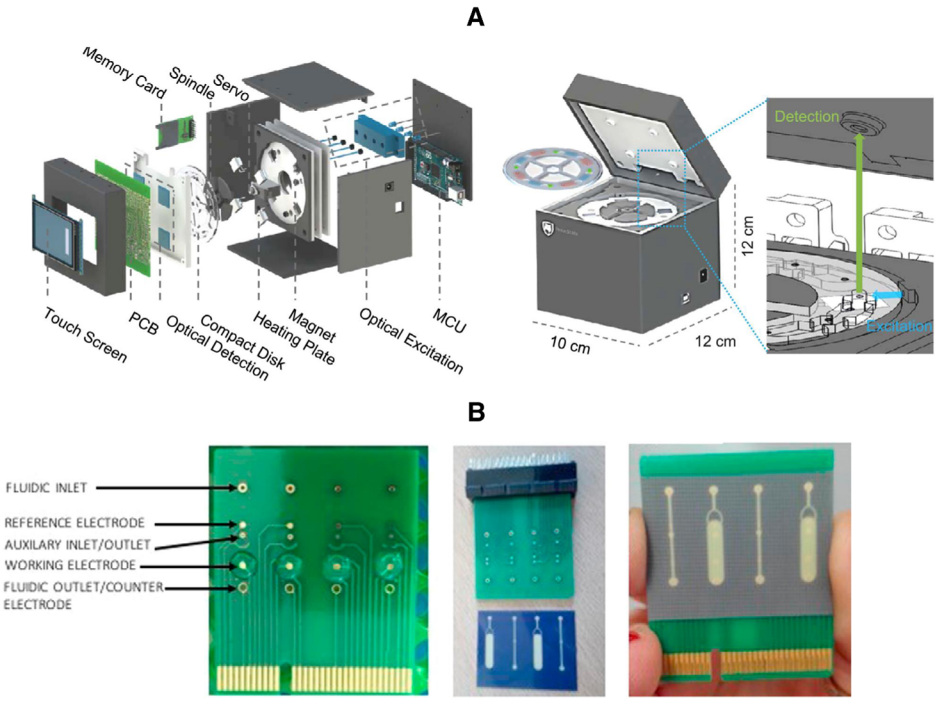

Figure 11. (A) The structure of the proposed sample-to-answer nucleic acid detection device, reprinted with permission from [84]. Copyright 2018 Elsevier; (B) the picture of the PCI Express connector interface of the proposed DNA diagnostic platform, reprinted with permission from [86]. Copyright 2019 Elsevier.

And its detection limit is ~0.5 parasites/μL, which fully meet the needs of malaria detection applications.

Temperature is a crucial factor in PCR, and reasonable control of the time and temperature stability of the three processes of denaturation (95°C), annealing (55°C), and extension (72°C) can achieve the shortest amplification time. Kaprou et al. designed a continuous μPCR device with short amplification time and low power consumption, including microfluidic device and embedded Cu microresistance heater with PCB as the substrate for precise heating of PCR process [87]. In order to better control the temperature of each stage, the heater is designed with three discrete hot zones, which are controlled by a temperature control unit consisting of a microcontroller, temperature sensor, digital-to-analog converter, and analog-to-digital converter. The analog-to-digital converter converts the temperature sensed by the temperature sensor into a digital signal and transmits it to the microcontroller for analysis. The microcontroller then controls the digital-to-analog converter to change the voltage across the heater to adjust the temperature. Kaprou et al. also used a detailed 3D modeling framework to analyze the residence time of DNA molecules in each hot zone to calculate the flow rate to achieve the best reaction environment. Ultimately, the device achieved a reduction in amplification reaction time of up to 2 min and its power consumption during operation was only 2.7 W.

In addition, Pawan et al. proposed a DNA diagnostic platform that uses peptide nucleic acid as a probe, which integrates microfluidic channels and characteristic sensors on the PCB to quantify DNA more efficiently [88]. There are four identical sensing electrodes on the PCB for easy repeatability studies. Connect the electrodes to the PCI Express connector interface (Fig. 11B) to facilitate the analysis of the detected experimental data through a slot-type electrical connection to an external instrument. The proposed device is capable of analyzing 5 μL samples with the concentration ranging from 0.1 to 100 μM with a continuous flow of 5 min, and a detection limit of 57 fM.

6 Concluding remarks

In this paper, we reviewed the studies about Lab-on-PCB for biomedical applications in recent years. We introduced the structure, performance, and advantages of Lab-on-PCB devices from four application directions, including cell analysis, biochemical analysis, immunoassay, and molecular diagnostics. Due to the mature manufacturing industry of the PCB, it is easy to integrate the sensor and the sensing signal processing system on the same PCB circuit, which can achieve mass production and reduce the costs. And the PCB has a high degree of integration, which has a great advantage in size compared with traditional sensing equipment. On the other hand, the PCB circuit can also be customized according to the actual needs of the user, so it can well meet the special needs of some sensor device designs. In addition, the recent emergence of flexible circuit materials has also promoted the development of wearable electrochemical sensors and make it possible to monitor human health indicators for a long time.

Although Lab-on-PCB has made good development in biomedical applications, in order to adapt to future development trends, we have proposed the following perspectives: (1) The minimum detection limit, sensitivity, and accuracy are important indicators for evaluating a sensor. Although

the detection performance of some Lab-on-PCBs is already comparable to commercial desktop instruments, there is still a large part that can only be qualitatively analyzed. Therefore, we also need to improve the existing lab-on-sensing technology or propose new and better sensing technologies to improve the sensitivity and accuracy of Lab-on-PCB detection. (2) With the rapid development of PCB technology, Lab-on-PCB wearable sensors have been put into biomedical applications, and the Lab-on-PCB sensors that are inserted into the body have also been tested on animals. These sensors can be used to detect human health indicators more accurately in the long term. Next, we can further reduce the size of Lab-on-PCB to improve its biocompatibility to pave the way for nanoscale biological detection devices that can implant in the human body in the future. (3) We can use the developed wireless communication technology to integrate multiple Lab-on-PCB to build a comprehensive platform for biochemical detection. Through comprehensive detection and analysis of different indicators, we can diagnose the disease more rapidly and accurately and provide treatment for the disease more reasonably. In addition, by combining big data technology and fifth generation wireless network communication technology, a larger Internet of medical Things can be constructed. Above all, we believe that through continuous development, Lab-on-PCB will play an increasingly important role in biomedical applications, providing a strong guarantee for people's health.

The authors have declared no conflict of interest.

7 References

[1] Ye, J., Letcher, S. V., Rand, A. G., *Electrophoresis* 2006, *62*, 1067–1086.

[2] Jiang, Y., Wu, J., *Electrophoresis* 2019, *40*, 2084–2097.

[3] Mishra, A. K., Mishra, S. B., Tiwari, A., in: Li, S., Singh, J., Li, H., Banerjee, I. A., (Eds.), *Biosensor Nanomaterials*, Wiley-VCH, Weinheim 2011, pp. 255–268.

[4] Özcan, H. M., Sezgintürk, M. K., *Biotechnol. Progr.* 2015, *31*, 815–822.

[5] Yao, J., Takei, M., *IEEE Sens. J.* 2017, *17*, 8196–8205.

[6] Kudo, H., Arakawa, T., Mitsubayashi, K., *Electr. Commun. Jpn.* 2014, *97*, 52–56.

[7] Xu, D., Huang X., Guo, J., Ma, X., *Biosens. Bioelectron.* 2018, *110*, 78–88.

[8] Sun, A. C., Hall, D. A., *Electrophoresis* 2018, *31*, 2–16.

[9] Lammerink, T. S. J., Spiering, V. L., Elewnspoek, M., Fluitman, J. H. J., den Berg, A., IEEE International Workshop on Micro Electro Mechanical Systems, San Diego, CA, 1996, 389–394.

[10] Talukder, N., Furniturewalla, A., Le, T., Chan, M., Hirday, S., Cao, X., Xie, P., Lin, Z., Gholizadeh, A., Orbine, S., Javanmard, M., *Biomed. Microdevices* 2017, *19*, 36.

[11] Ninno, A. D., Errico, V., Bertani, F. R., Businaro, L., Bisegna, P., Caselli, F., *Lab Chip* 2017, *17*, 1158–1166.

[12] Mcgrath, J. S., Honrado, C., Spencer, D., Horton, B., Bridle, H. L., Morgan, H., *Sci. Rep.* 2017, *7*, 2601.

[13] Cheung, K., Gawad, S., Renaud, P., *Cytom. A* 2005, *65*, 124–132.

[14] Fu, Y., Yuan, Q., Guo J., *Microfluid. Nanofluid.* 2017, *21*, 20.

[15] Guo, J., Chen, L., Ai, Y., Cheng, Y., *Electrophoresis* 2015, *36*, 737–743.

[16] Guo, J., Li, C. M., Kang, Y., *Biomed. Microdevices* 2014, *16*, 681–686.

[17] Xu, G., Cheng, C., Liu, Z., Yuan, W., *Adv. Mater.* 2019, 4, *7*, 1800658.

[18] Khan, Y., Thielens, A., Muin, S., Ting, J., Baumbauer, J., Arias, A. C., *Adv. Mater.* 2019, 1905279 .

[19] Ma, Y., Zhang, Y., Cai, S., Han, Z., Liu, X., Wang, F., Cao, Y., Wang, Z., Li, H., Chen, Y., Feng, X., *Adv. Mater.* 2019, 1902062.

[20] Vasilakis, N., Papadimitriou, K. I., Evans, D., Morgan, H., Prodromakis, T., *2016 IEEE Healthcare Innovation Point-Of-Care Technologies Conference (HI-POCT)*, Cancun, Mexico, 2016, 126–129.

[21] Cardosi, M. F., Birch, S. W., Smith, B. M., Johannsson, A., *Electroanalysis* 1989, *1*, 297–304.

[22] Hong, D., Joung, H. A., Lee, D. Y., Kim, S., *Sens. Actuators B Chem.* 2015, *221*, 1248–1255.

[23] Cheng, S. B., Skinner, C. D., Taylor, J., Attiya, S., *Anal. Chem.* 2001, *73*, 1472–1479.

[24] La Belle, J. T., Gerlach, J. Q., Svarovsky, S., Joshi, L., *Anal. Chem.* 2007, *79*, 6959–6964.

[25] Mir, M., Homs, A., Samitier, J., *Electrophoresis* 2009, *30*, 3386–3397.

[26] Pardo, W. A., Mir, M., Samitier, J., *Electrophoresis* 2015, *36*, 1905–1911.

[27] Jenkins, D. M., Kubota, R., Dong, J., Li, Y., Higashiguchi, D., *Biosens. Bioelectron.* 2011, *30*, 255–260.

[28] Garbarino, F., Minero, G., Rizzi, G., Fock, J., Neumann, F., Madaboosi, N., Asalapuram, P., Nilsson, M., Hanse, M. F., *Biosens. Bioelectron.* 2019, *142*, 111485.

[29] Zou, F., Ruan, Q., Lin, X., Zhang, M., Song, Y., Zhou, L., Zhu, Z., Lin, S., Wang, W., Yang, C. J., *Biosens. Bioelectron.* 2018, *126*, 551–557.

[30] Huang, X., Xu, D., Chen, J., Liu, J., Li, Y., Song, J., Ma, X., Guo, J., *Analyst* 2018, *22*, 5339–5351.

[31] Wang, X., Lin, G., Cui, G., Zhou, X., Liu, G. L., *Biosens. Bioelectron.* 2017, *90*, 549–557.

[32] Tan, F., Wang, T., Wang, H., Zheng, Y., *Electrophoresis* 2019, *40*, 1230–1244.

[33] Ge, J., Gong, Z., Chen, J., Nguyen, J., Yang, Z., Wang, C., Sun, Y., *IEEE Trans. Biomed. Eng.* 2014, *61*, 2823–2829.

[34] Wang, K., Sui, D., Wang, W., Yuan, Y., Zuo, W., *Annual International Conference of the IEEE Engineering in Medicine and Biology Society*, San Diego, CA, 2012, 118–121.

[35] Guo, J., Pui, T. S., Rahman, A. R., Kang, Y., *Electrophoresis* 2013, *34*, 417–424.

[36] Guo, J., Chen, L., Huang, X., Li, C. M., Ai, Y., Kang, Y., *Electrophoresis* 2015, *36*, 420–423.

[37] Shi, D., Guo, J., Chen, L., Xia, C., Yu, Z., Ai, Y., Li, C. M., Kang, Y., Wang, Z., *Electrophoresis* 2015, *36* 1854–1858.

[38] Park, K., Suk, H. J., Akin, D., Bashir, R., *Lab Chip* 2009, *9*, 2224–2229.

[39] Jun-Chau, C., Ali, A., Erh-Chia, Y., Alison, N. K., Mekhail, A., Ali, M. N., *Lab Chip* 2018, *18*, 2065–2076.

[40] Guo, J., Ai, Y., Cheng, Y., Li, C. M., Kang, Y., Wang, Z., *Electrophoresis* 2015, *36*, 1862–1865.

[41] Chen, L., Guo, J., *Electrophoresis* 2015, *36*, 1859–1861.

[42] Zhao, Y., Zhang, W., *Electrophoresis* 2018, *40*, 1140–1143.

[43] Yao, J., Zhu, G., Zhao, T., Takei, M., *Electrophoresis* 2018, *40*, 1166–1177.

[44] Guo, J., Li, H., Chen, Y., Kang, Y., *IEEE Sens. J.* 2014, *14*, 2112–2117.

[45] Guo, J., Kang, Y., Ai, Y., *IEEE Trans. Dielectr. Electr. Insul.* 2015, *22*, 1439–1443.

[46] Guo, J., Huang, X., Ai, Y., *Anal. Chem.* 2015, *87*, 6516–6519.

[47] Nikshoar, M.S., Khosravi, S., Jahangiri, M., Zandi, A., Miripour, Z. S., Bonakdar, S., Abdolahad, M., *Biosens. Bioelectron.* 2018, *118*, 51–57.

[48] Senevirathna, B., Lu, S., Dandin, M., Basile, J., Smela, E., Abshire, P., *Biosens. Bioelectron.* 2019, *142*, 111501.

[49] Rose, D. P., Ratterman, M. E., Griffin, D. K., Hou, L., Lounghnane, N. K., Naik, R. R., Hagen, J. A., *IEEE Trans. Biomed. Eng.* 2015, *62*, 1457–1465.

[50] Na, J., Hong, M. H., Choi, J. S., Kwak, H., Song, S., Kim, H., Chae, Y., Cheong, E., Lee, J. H., Lim, Y., Choi, H. J., *Nano Lett.* 2019, *19*, 2291–2298.

[51] Nemiroski, A., Christodouleas, D. C., Hennek, J. W., Kumar, A. A., Maxwell, E. J., Fernández-Abedul, M. T., Whitesides, G. M., *Proc. Natl. Acad. Sci. USA*, 2014, *111*, 11984–11989.

[52] Martin, A., Kim, J., Kurniawan, J. F., Sempionatto, J. R., Moreto, J. R., Tang, G., Campbell, A. S., Shin, A., Lee, M. Y., Liu, X., Wang, J., *ACS Sens.* 2017, *2*, 1860–1868.

[53] Rocchitta, G., Secchi, O., Alvau, M., Farina, D., Bazzu, G., Calia, G., Migheli, R., Desole, M. S., O'Neill, R. D., Serra, P. A., *Anal. Chem.* 2013, *85*, 2–8.

[54] Ozcan, S., *EMBO J.* 1998, *17*, 2566–2573.

[55] Saa, L., Pavlov, V., *Small* 2012, *8*, 3448-3448.

[56] Mcminn, A., Lee, S., *J. Phycol.* 2018, *54*, 410–418.

[57] Zhu, X., Yuan, S., Ju, Y., Yang, J., Zhao, C., Liu, H., *Anal. Chem.* 2019, *91*, 10764–10771.

[58] Schazmann, B., Morris, D., Slater, C., Btephen, B., Fay, C., Reuveny, R., Mouna, N., Diamond, D., *Anal. Methods* 2010, *2*, 342–348.

[59] Anastasova, S., Kassanos, P., Yang, G. Z., *Biosens. Bioelectron.* 2017, *102*, 668–675.

[60] Nyein, H. Y. Y., Tai, L. C., Ngo, Q. P., Chao, M., Zhang, G. B., Gao, W., Bariya, M., Bullock, J., Kim, H., Fahad, H. M., Javey, A., *ACS Sens.* 2018, *3*, 944–952.

[61] Gao, W., Emaminejad, S., Nyein, H. Y. Y., Challa, S., Chen, K., Peck, A., Fahad, H. M., Ota, H., Shiraki, H., Kiriya, D., Lien, D. H., Brooks, G. A., Davis, R. W., Javey A., *Nature* 2016, *529*, 509–514.

[62] Emrich, H. M., Stoll, E., Friolet, B., Colombo, J. P., Richterich, R., Rossi, E., *Pediatr. Res.* 1968, *2*, 464–478.

[63] Salvo, P., Francesco, F. D., Costanzo, D., Ferrari, C., Trivella, M. G., Rossi, D. D., *IEEE Sens. J.* 2010, *10*, 1557–1558.

[64] Coyle, S., Morris, D., Lau, K. T., Diamond, D., Taccini, N., Costanzo, D., Salvo, P., Francesco, F. D., Trivella, M. G., Porchet, J. A., Luprano, J., *3rd International Conference on Pervasive Computing Technologies for Healthcare*, London, UK, 2009.

[65] Guo, J., *Anal. Chem.* 2016, *88*, 11986–11989.

[66] Guo, J., *Anal. Chem.* 2017, *89*, 8609–9613.

[67] Aymerich, J., Márquez, A., Terés, L., Muñoz-Berbel, X., Jiménez, C., Domínguez, C., Serra-Graells, F., Dei, M., *Biosens. Bioelectron.* 2018, 736–742.

[68] Mohammed, M. I., Desmulliez, M. P. Y., *Lab Chip* 2011, *11*, 569–595.

[69] Banerjee, R., Jaiswal, A., *Analyst* 2018, *143*, 1970–1996.

[70] Lee, J., Kwon, J. H., Kim, H. T., Cho, H. B., Cha, Y. J., *Nanoscale* 2019, *11*, 18282–18289.

[71] Lee, J., Kwon, J. H., Kim, H. T., Cho, H. B., Cha, Y. J., Lee, J. H., Kim, R., Shin, J., Cha, Y. J., Heo, M., *Nanoscale* 2017, 16476–16484.

[72] Sanjay, S. T., Fu, G., Dou, M., Xu, F., Liu, R., Qi, H., Li, X. *Analyst*, *140*, 7062–7081.

[73] Lee, J., Choi, Y. S., Lee, Y., Lee, H. J., Lee, J. N., Kim, S. K., Han, K. Y., Cho, E. C., Park, J. C., Lee, S.S., *Anal. Chem.* 2012, *1415*, 8629–8635.

[74] Bonilla, D., Mallen, M., Rica, R. D., Sanchez, C. F., Baldi, A., *Anal. Chem.* 2019, *83*, 1726–1731.

[75] Simons, S. S. H., Cillessen, A. H. N., De, W. C., *Dev. Psychobiol.* 2016, *59*, 217–224.

[76] Prete, A., Yan, Q., Al-Tarrah, K., Akturk, H. K., Prokop, L. J., Alahdab, F., Foster, M. A., Lord, J. M., Karavitaki, N., Wass, J. A., Murad, M. H., Arlt, W., Bancos, I., *Clin. Endocrinol.* 2018, *89*, 554–567.

[77] Khan, M. S., Misra, S. K., Wang, Z., Daza, E., Schwartz-Duval, A. S., Kus, J. M., Pan, D., Pan, D., *Anal. Chem. 89*, 2107–2115.

[78] Nagy, B., Al-Rawhani, M. A., Cheah, B. C., Barrett, M. P., Cumming, D. R. S., *ACS Sens.* 2018, *3*, 953–959.

[79] Kim, C., Hoffmann, G., Searson, P. C., *ACS Sens.* 2017, *2*, 766–772.

[80] Novo, P., Chu, V., Conde, J. P., *Biosens. Bioelectron.* 2014, *57*, 284–291.

[81] Roper, M. G., Easley, C. J., Landers, J. P., *Anal. Chem.* 2005, *77*, 3887–3894.

[82] Zhang, C., Xu, J., Ma, W., Zheng, W., *Biotechnol. Adv.* 2006, *24*, 243–284.

[83] Asiello, P, J., B, Antje, J., *Lab Chip* 2011, *11*, 1420–1430.

[84] Park, S., Zhang, Y., Lin, S., Wang, T. H., Yang, S., *Biotechnol. Adv.* 2011, *29*, 830–839.

[85] Jangam, S. R., Agarwal, A. K., Sur, K., Kelso, D. M., *Biosens. Bioelectron.* 2013, *42*, 69–75.

[86] Choi, G., Prince, T., Miao, J., Cui, L., Guan, W., *Biosens. Bioelectron.* 2018, *115*, 83–90.

[87] Kaprou, G. D., Papadopoulos, V., Papageorgiou, D. P., Kefala, I., Papadakis, G., Gizeli, E., Chatzandroulis, S., Kokkoris, G., Tserepi, A., *Anal. Bioanal. Chem.* 2019, *411*, 5297–5307.

[88] Pawan, J., Joshua, R., Anna, R., Estrela, P., Moschou, D., *Biosens. Bioelectron.* 2018, *123*, 244–250.

